



Photocatalytic activity of sol–gel-derived mesoporous TiO₂ thin films for reactive orange 16 degradation

Suhas R. Patil^{a,b}, U.G. Akpan^{a,c}, B.H. Hameed^{a,d,*}

^aSchool of Chemical Engineering, Engineering Campus, Universiti Sains Malaysia, Nibong Tebal, Penang 14300, Malaysia
Fax: +6045941013; email: chbassim@eng.usm.my

^bDepartment of Physics, Dr Annasaheb G.D. Bendale Mahila Mahavidyalaya, Jalgaon, M.S 425 001, India

^cChemical Engineering Department, Federal University of Technology, P.M.B. 65, Minna, Nigeria

^dChemical Engineering Department, College of Engineering, King Saud University, P.O. Box 800, Riyadh 11421, Saudi Arabia

Received 3 August 2013; Accepted 28 November 2013

ABSTRACT

This study investigates the photocatalytic activity of sol–gel-derived mesoporous TiO₂ thin films for reactive orange 16 (RO16) degradation. Both surfactant- and non-surfactant-assisted sols were prepared and coated on different glass slides. The prepared catalysts were characterized by X-ray diffraction, surface scanning electron microscopy, UV–vis transmittance spectra, and nitrogen adsorption/desorption isotherms for their properties, while the photocatalytic activities of the TiO₂ thin films were evaluated in the degradation of RO16. The surfactant-assisted films showed surface uniformity, reduced particle size, and high photocatalytic activity compared to non-surfactant assisted films. The effects of withdrawal speed on films' transparency and the number of coatings on UV light absorption and their photocatalytic activities are systematically explained for the surfactant-assisted films. Though there was a continuous increase in the efficiency of the mass of TiO₂ per unit area and UV light absorption with the increase in the number of dip-coatings, any further increase in the number of coatings beyond five did not show any significant increase in the degradation rate, indicating that further coatings resulted in the blocking of middle pores.

Keywords: Sol–gel; Mesoporous TiO₂; Thin film; UV light absorption; Degradation; Dye

1. Introduction

Titanium dioxide is widely used in every field, such as dye-sensitized visible light material [1], self-cleaning material [2], gas sensing devices [3], biomaterials [4], and electrochemical electrode and capacitors [5]. Also, TiO₂-based photocatalyst is promising in

environmental applications, such as photocatalytic degradation of pollutants [6–9]. In photocatalytic application, TiO₂ is extensively used in either aqueous [10–12] or fixed bed media [13,14]. Aqueous media operation using powder photocatalysts is rather demanding and time-consuming in the separation of the photocatalytic materials. Above all, loss of photocatalysts is experienced during separations and reuse process; but, this problem can be avoided in thin films as the photocatalysts are firmly fixed to their supports.

*Corresponding author.

However, in the fixed bed media the reaction occurs at the liquid–solid interface; hence, only a part of the catalyst is in contact with the reactant. Therefore, the overall rate may be limited by mass transport of the pollutant to the catalyst surface [15]. Another problem, besides the lack of good contact between reactants and catalyst, is insufficient exposure of the catalyst to irradiation through the whole interior of the reactor [16] since only one side of the film is exposed to irradiation.

Crystalline phase, specific surface area, and porous structure of the catalyst are distinctive features which determine the activity of TiO₂ [13]. However, to enhance a good contact between reactants and catalyst, and efficient exposure of the catalyst to irradiation, various approaches have been reported in literature, such as synthesis of the porous film of the catalyst [13,17], enhancement in the surface roughness [18–20], and increase in the thin film thickness [13,21–23]. The porous films of TiO₂ may be more effective when the photodegradation mechanism includes reactants adsorbed on the surface of the catalyst. Furthermore, the mesoporosity may ensure fast transport of O₂ and H₂O, which are viable for the photocatalytic degradation of deposited layers of dirt and can be significantly hindered due to the compactness of those layers [13,24]. On the other hand, in general, the hydrophilicity of a thin film surface is strongly influenced by its geometric structure [20,25].

Reports revealed that a variety of surfactants/polymer templating techniques have successfully been used in the sol–gel preparation of mesoporous TiO₂ thin films using Tween-20 [26,27], Tween-80 [28], polyethylene glycol [29,30], diethylene glycol [30], Brij 56 and Triton X-100 [21,27], Pluronic F127 [17,20,21], and Pluronic P123 [31]. Surfactants or polymer templates are considered to be the potential structure-directing agents to give: (1) the mesoporous film structure, which can improve the catalytic properties of the catalyst, as well as transparency and (2) structure stability [13]. It has previously been reported that a comparative study had been carried out to determine the best pore-generating agent between Pluronic F127, Brij 56, and Triton X-100 [17,21]. The results of the study showed that Pluronic F127 is excellent in this regard. Earlier studies revealed that the use of surfactant in synthesizing TiO₂ thin film not only help in controlling mesoporosity but also enhance the surface roughness and hydrophilicity of the film [13,17,20].

Another important factor influencing photocatalytic activity of TiO₂ film is thickness. In case of sol–gel dip-coating, the thickness of film can be controlled by either changing withdrawal speed or alternate coating/heating cycles. It has been reported that increase

in film thickness through repeated dip-coating process can increase the amount of coated material on the substrate and linearly enhance the photocatalytic activity of the TiO₂ film [19,21,23,26,32]. Nevertheless, it has also been reported that increase in the TiO₂ film thickness resulted in negligible increase in the photocatalytic activity of the thin film for the degradation of methylene blue [33]. Yaghoubi et al. [19] showed that the activity of TiO₂ film increased up to four alternate coatings which is consistent with previous reports by Cernigoj et al. [21] and Chen et al. [26], but the UV–vis transmittance spectra is entirely inconsistent with them. However, Cernigoj et al. [21] indicated that the band gap decreased with increasing number of coating/heating cycle, which is again inconsistent with recent report [13]. Chen et al. [26] showed that as the number of dip-coatings increase, the transmittance decrease at the wavelength ranging from 300 to 375 nm, which obeys the Beer–Lambert law.

The report of Yu et al. [34] on the “photocatalytic activity of nanometer TiO₂ thin films prepared by the sol–gel method” claimed that there is a proportionate increase in film thickness with increase in the number of dip-coating/heating cycles. They also observed that as the cycle increased from 1 to 15, the degradation rate constant for methyl orange increased from 0.0189 to 0.0301 min⁻¹. Nevertheless, it is apparent that there must be a certain number of coatings beyond which further dip-coating may not enhance the activity of the TiO₂ thin film. Furthermore, as it is depicted from the results of the present study, excessive number of coatings may result in cracking and eventual removal of substrate from the film during reaction which will act to diminish its activity in the subsequent reaction.

It was therefore necessary to investigate the activities of various mesoporous TiO₂ thin films’ thickness with varying withdrawal speed/alternate coatings, and this present study was set out to undertake this. The model pollutant used to test the degradation potential of the mesoporous TiO₂ thin films is an azo dye, reactive orange 16(RO16).

It must also be noted that the combined effect of the variation in the UV–vis light absorption and thickness of mesoporous films on their photocatalytic performance markedly depends on the system tested. Therefore, the present study was organized to optimize the withdrawal speed, alternate coatings/thickness of films and their light absorption, and the correlation of these properties with the photocatalytic activity in the degradation of an azo dye, reactive orange 16 (RO16). In the previous work [13], thin films were prepared from strong acidic sol, but in the present study thin films were prepared from a weak acidic sol, and their photocatalytic activities evaluated. The

effect of inner layer porosity in the degradation of the model dye and the characterizations of the photocatalyst-/thin film-coated TiO₂ are also discussed.

2. Materials and methods

2.1. Chemicals

The chemicals in this study were used as purchased: Titanium (IV) isopropoxide (Ti(OiPr)₄, 98% Aldrich), absolute ethanol (EtOH, Merck), ethyl acetoacetate (EAA, 98% Merck), 2-methoxyethanol (MeO (CH₂)₂OH, >99% Sigma-Aldrich), tetraethoxysilane (TEOS, 99% Merck), concentrated HNO₃ (65% Merck), RO16 dye (C.I. = 17,757, dye content ca. 50% Sigma-Aldrich), Pluronic F127 (Surfactant, Sigma), and deionized water.

2.2. Preparation of the sol and glass slide/SiO₂/TiO₂ films

Prior to use, the glass slides were cleaned with a solution containing 5 mL concentrated HNO₃ and 200 mL distilled water in ultrasonic bath for 20 min, and then with ethanol to remove possible stains from the glass slides. First a dense SiO₂ barrier layer was deposited on the glass slides (25 × 70 × 1 mm) to avoid diffusion of Na⁺ ions from the glass substrate to the TiO₂ film during calcination and possible inhibition of photocatalytic activity [13,17] as follows: the SiO₂ sol was prepared from a TEOS precursor, ethanol ($n(\text{EtOH})/n(\text{Si}) = 6.47$), HNO₃ ($n(\text{HNO}_3)/n(\text{Si}) = 0.44$), and water ($n(\text{H}_2\text{O})/n(\text{Si}) = 8.06$). After 2 h of mixing, the resulting solution was used for SiO₂ barrier layer synthesis by the dip-coating technique with pulling speed of 10 cm min⁻¹ [20]. All SiO₂ coatings were produced by a single dipping and calcination at 500°C for 30 min.

The TiO₂ films were prepared by sol-gel dip-coating method according to high temperature sol film [20]. In particular, Ti(OiPr)₄ was added to EAA ($n(\text{EAA})/n(\text{Ti}(\text{OiPr})_4) = 1$) at room temperature under vigorous stirring. After 20 min, the prepared solution was dissolved in 2-methoxyethanol ($n(\text{Ti}(\text{OiPr})_4)/n(\text{MeO}(\text{CH}_2)_2\text{OH}) = 0.075$) and the resulting solution was subsequently aged at room temperature for at least 3 h. The surfactant Pluronic F127 was used as pore-generating agent with 10 wt.% of total titania sol. All TiO₂ thin films prepared were immediately dried synthetically and then calcined at 500°C for 30 min. The amount of TiO₂ per unit area was increased by repeating the dip-coating and heat-treatment cycles up to six times. The transparent TiO₂ films were deposited on both sides of SiO₂ pre-coated glass slides with varying withdrawal speed (from 10 to 50 cm min⁻¹) by sol-gel dip-coating method as previously described

[20]. The TiO₂ powder samples used for X-ray diffraction (XRD) and Brunauer–Emmet–Teller (BET) investigations were prepared by casting the dip-coating sols on a clean glass plate and dried synthetically until all solvent was removed. After solvent evaporation, the remaining thick films were scraped from the glass plate and the collected powder was calcined at 500°C for 2 h. It is important to note here that the powder sample would have been calcined for 30 min as in the case of thin film, but preliminary investigations showed that for dense powder sample, 30 min was outright insufficient to remove the surfactant from the TiO₂ sample. Therefore, to have TiO₂ sample without the polymeric effect of surfactant, 2 h was sufficient for the calcination of the dense powder sample. Actually, calcinations were carried out at 30, 60, 90 and 120 min, but at 30 min calcination of the powder sample a dark sooty material (which indicates that the surfactant is not removed) was obtained which gradually cleared up as time progressed to a fine TiO₂ powder color at 2 h.

2.3. Characterization of catalyst

The transmittance spectra of the various TiO₂ films were recorded on a Shimadzu UV-1700 PharmaSpec UV-vis spectrophotometer. XRD patterns of the films and powder samples were measured by D8 Advanced X-ray solution with an alpha 1 configuration using CuK α radiation (1.5406 Å) in a wide-angle range (2 θ) from 20° to 60° with a step angle of 0.0342°. The average particles sizes were determined from the Scherrer's equation [20] ($0.94\lambda/\beta\cos\theta$) using the broadening of the (1 0 1) anatase peak reflection, where λ is the wavelength of X-ray, θ is the diffraction angle, and β is the full width at half maximum intensity of the peak. Nitrogen adsorption/desorption isotherms of the synthesized TiO₂ powder samples prepared with/without surfactant were collected on ASAP 2020 V3.02 H Micromeritics surface area and porosity analyzer at 77 K. The BET surface area was calculated from the linear part of the BET plot. The pore size distribution (PSD) and average pore volume plots were obtained by using the Barret–Joyner–Halenda (BJH) model. Field emission scanning electron microscopy (FE-SEM) measurements were carried out by the means of a Field Emission Zeiss SUPRA 35VP instrument. Top surface images were acquired by adopting accelerating voltage at 5 kV.

2.4. Photocatalytic activities of the films

The photocatalytic activities of the various films were performed at room temperature (27 ± 1°C) in a 400 mL jacketed glass reactor fitted with a 9W 5-inch long-Philips (PL-S 9 W/10/2P Hg, maximum

absorption wavelength at 254 nm) bulb made in Poland. Then, 225 mL of the aqueous solution of 25 mg L⁻¹ RO16 dye concentration was poured into the photoreactor (which was placed in a black box to shield the researcher from direct contact with the UV light); after the addition of six films of TiO₂ with Teflon glass slide holder to it, the light was switched on. It must be noted that the glass slide holder was made in a circular form, so that the glass film will surround the bulb and, the irradiation would be normal to the film. The reactor content was agitated at 530 rpm using a magnetic stirrer, and oxygen was introduced into the reaction medium. Samples were withdrawn from the irradiated solution at preset time intervals and analyzed for the concentration of RO16 in solution at 493 nm (the dye's maximum absorption wavelength).

3. Results and discussion

Preliminary studies (results not shown) revealed that non-surfactant-assisted TiO₂ coatings on the thin glass film were partially transparent and were not as effective as the surfactant assisted TiO₂ coatings; so, further investigations using non-surfactant TiO₂ thin glass films were not carried out. Again, dense TiO₂ powder prepared and synthetically dried in the same manner as that of the thin films had some soots in it after 1-h calcination at 500°C. The sample was void of soots when it was calcined for 2 h at 500°C; hence, 2 h was slated as the duration for the calcination of the powder samples used for characterization where thin films cannot be used.

3.1. UV–vis transmittance spectra of the films

The UV–vis transmittance spectra of the TiO₂ films prepared on SiO₂ precoated glass slides with varying withdrawal speeds from 10 to 50 cm min⁻¹ for one coating and one to six alternate coatings for 20 cm min⁻¹ withdrawal speed are shown in Fig. 1(a) and (b), respectively. The SiO₂ precoated glass slide shows a very high transmittance over the whole near UV and visible light region. In contrast, there was a remarkable reduction in transmittance in the UV range (300–380 nm) due to the introduction of TiO₂ coatings (Fig. 1(a) and (b)). Fig. 1(a) clearly shows that the absorption of light in the UV range increased with the increase in withdrawal speed up to 40 cm min⁻¹. Further increase in the withdrawal speed to 50 cm min⁻¹ resulted in a decrease in the absorption of light in the UV range, suggesting that there may be a crack on the film or that some mass of TiO₂ could have been

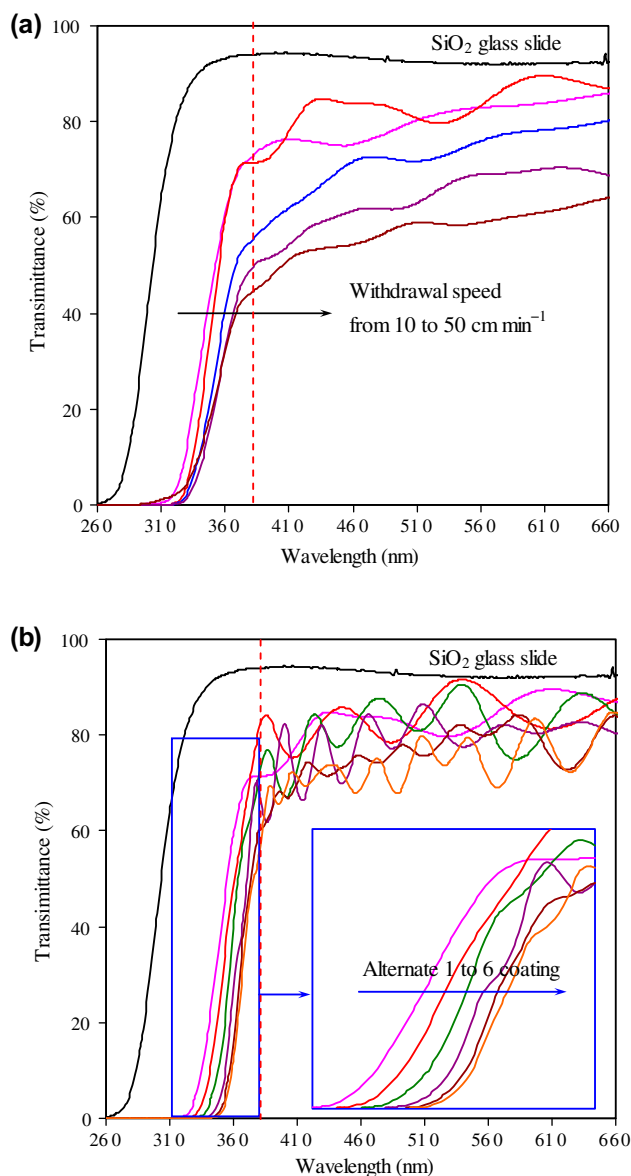


Fig. 1. UV–vis transmission spectra of TiO₂ films deposited by dip-coating technique: (a) withdrawal speed from 10 to 50 cm min⁻¹ and (b) one to six alternate coatings at withdrawal speed of 20 cm min⁻¹ on SiO₂ coated glass slide.

removed during washing of the film, thus paving way for free passage of light that should have been absorbed. However, the film prepared with 20 cm min⁻¹ withdrawal speed shows a very high transparency (over 80%) in the whole visible light region and even higher than that of other coatings prepared by varying withdrawal speeds. Physical or visual examination of the films after calcinations revealed that thin films prepared at higher withdrawal speeds turned milky and this might inhibit the transmission of light through them. At a withdrawal speed of 20 cm min⁻¹,

the mist disappeared, films were more transparent than others, and the mass of TiO_2 per unit area in such films increased with increase withdrawal speeds. Further works carried out with withdrawal speed of 20 cm min^{-1} were not only based on transparency, but the surface morphology of such film is uniform and crack-free.

When it became apparent that 20 cm min^{-1} withdrawal speed was the best, it was, therefore, used for the preparation of TiO_2 thin films up to six alternate coatings. Fig. 1(b) depicts that the absorption of light in the UV range increased with increase number of alternate coatings. However, observations of Fig. 1(b inset) reveal that the rate of increase in UV light absorption decreases with the number of alternate coatings, and became smaller between fifth and sixth coatings.

The transparency of one to six coatings over the whole visible light region (after 390 nm wavelength) is as high as about 70%, even after five or six coatings the transparency of the films was higher than those with a single coating prepared by varying withdrawal speeds. In the wavelength range of 390–660 nm, bands were observed and these were due to interfering color from the films. The amplitudes of the bands decreased with increase in the number of alternate TiO_2 coatings. Moreover, it was observed from Fig. 1(b) that the number of interference peaks increased with the number of alternate coating/heating cycles, suggesting that the films are multi-layers with increasing mass per unit area. In addition, each successive number of coatings did not significantly affect transmittance in the visible light region. The contributing effects of the number of alternate TiO_2 coatings on the degradation of pollutant were further confirmed from the photocatalytic degradation of the RO16 dye. The observed performance highlights a direct correspondence between the number of alternate TiO_2 coatings with its structural morphology and the photocatalytic degradation of the dye RO16 dye.

3.2. XRD investigations

Fig. 2 shows the XRD patterns of (a,b,c) TiO_2 films dip-coated on precoated SiO_2 glass slide substrate and (d,e) TiO_2 powder sample synthesized with and without surfactant. The XRD patterns of films (a,b,c) show weak anatase phase characteristic peak at $2\theta = 25.4^\circ$ (101). It has been reported that below certain number of coatings, the XRD peaks were too faint to be identified due to the small amount of TiO_2 coated onto the substrate [35]. For more accurate crystalline phase analysis, powder samples prepared from thick film were analyzed by the XRD instrument as shown in Fig. 2(d,e). Evidently, all the peaks belong to anatase

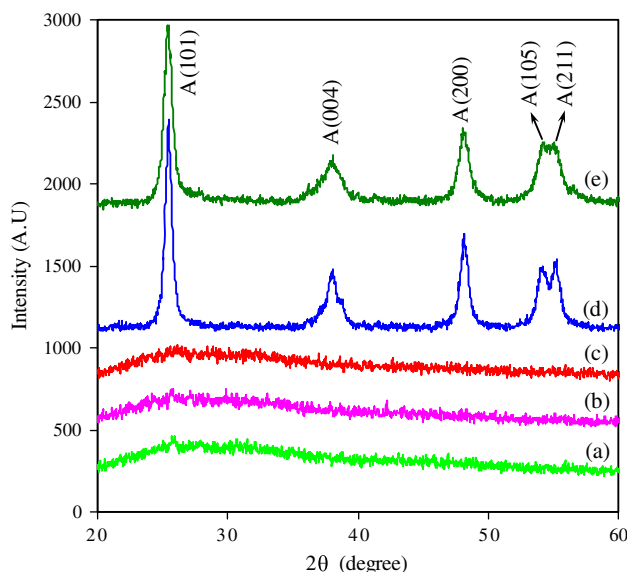


Fig. 2. XRD pattern of TiO_2 coatings prepared on SiO_2 coated glass slide substrate: (a) one coating without surfactant at withdrawal speed of 10 cm min^{-1} , (b) one coating with surfactant at withdrawal speed of 10 cm min^{-1} , (c) five coatings with surfactant at withdrawal speed of 20 cm min^{-1} , (d) TiO_2 powder sample prepared without surfactant and (e) TiO_2 powder sample prepared with surfactant.

phase and appeared at $2\theta = 25.4^\circ$, 38.1° , 48° , 54.1° , and 55.2° corresponding to (101), (004), (200), (105), and (211) reflections, respectively, no additional peaks belonging to rutile or brookite phases are observed in any of the TiO_2 powder samples. It is generally known that among the crystalline phases of TiO_2 , anatase is photocatalytically most active [36].

The average crystallite size was determined from the Scherrer's equation using the broadening of the (101) anatase peak of the XRD powder samples (d,e). The reduction in peak intensity and increase in broadness of the diffraction peaks on incorporation of surfactant into titania sol suggest a decrease in the crystallite size (from 16.5 to 12.9 nm). This result indicates that the use of non-ionic surfactants can inhibit large size crystallite growth [13,27].

3.3. BET investigations

Fig. 3 depicts N_2 adsorption/desorption isotherms of TiO_2 powders prepared (a) without surfactant and (b) with surfactant and BJH PSD (inset). The adsorption/desorption isotherms of (a) powder indicates that the material could belong to type II isotherms with negligible type. H_2 hysteresis loop between 0.45 and 0.7 relative pressure (P/P_0) range, which further indicates that the material is slightly mesoporous.

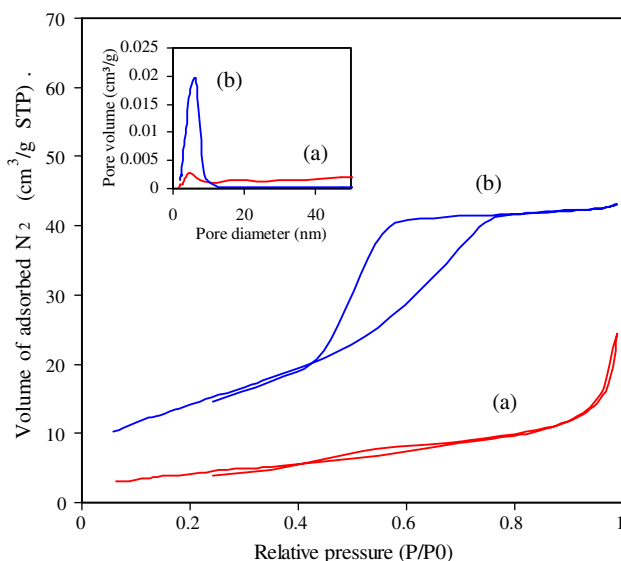


Fig. 3. N_2 adsorption–desorption isotherms and inset BJH PSD of with (b) and without surfactant (a) TiO_2 powder samples.

However, the adsorption/desorption isotherm of (b) the powder is clearly indicating type IV isotherms with type H2-hysteresis loop in the relative pressure (P/P_0) range of 0.45–0.8, which is a typical characteristic of a mesoporous material, according to the International Union of Pure and Applied Chemistry classification [37]. It is clearly seen from both (a) and (b) isotherms that upon the incorporation of surfactant into the sol, there is an increase in N_2 adsorption, indicating that the integration of the surfactant into the sol not only leads to an increase in BET surface area (from 15 to $53 \text{ m}^2 \text{ g}^{-1}$) but also to an enlargement of the PSD (Fig. 3 inset) [13].

Fig. 3 (inset) shows PSD curves determined from the N_2 adsorption/desorption isotherms. PSDs of the synthesized (a) and (b) TiO_2 powder samples have been determined using the desorption branch of the nitrogen adsorption–desorption isotherms by the BJH model. In both cases, one maximum point was observed which is slightly shifted to higher values and becomes more intense and broader with the incorporation of the surfactant into the sol. Such changes signify an increase in the pore size (from 4.8 to 6.4 nm), pore volume (from 0.003 to $0.02 \text{ m}^3 \text{ g}^{-1}$), and size distribution of pores. The wider distributions of mesopores in case of surfactant-assisted TiO_2 coating played adsorptive roles and RO16 dye molecules were adsorbed in the mesoporous TiO_2 coating surroundings, which was favorable to increase the photocatalytic activity of the film.

3.4. FE-SEM investigations

The surface morphology of the sol–gel dip-coated TiO_2 film with different withdrawal speeds was studied by FE-SEM. The SEM images with equal magnification reveal that the surface morphology of the TiO_2 film alters with increase in withdrawal speed. Fig. 4(a) is a SEM image of TiO_2 film prepared without surfactant, whereas images Fig. 4(b–f) are the surfactant-assisted sol–gel dip-coated TiO_2 films. Fig. 4(a) and (b) images are of the same withdrawal speed (10 cm min^{-1}) but different surface morphologies. Fig. 4(a) shows that there are some places with stacks of agglomerates of TiO_2 nano particles; several nano particles appeared to fuse together to form agglomerates (see yellow circle), although the same film at other places shows some unaided TiO_2 nano particles (see red circle) having a size of around 20–25 nm. Nevertheless, Fig. 4(b) constituted a uniform dispersion of spherical-shaped TiO_2 nano particles in the size range of 10–12 nm. These results indicate that the introduction of surfactant into the sol not only induces homogeneity in the film, but also assists in reducing the size of TiO_2 nano particles, which is favorable for the enhancement of the photocatalytic activity of the TiO_2 film. Figs. 4(b) and (c) show the surface morphology of TiO_2 film dip-coated with different withdrawal speeds, 10 and 20 cm min^{-1} , respectively. A closer observation of the SEM (b) and (c) images of the TiO_2 film revealed that the surface morphology of both films is unique. Figs. 4(d) and (e) show the surface morphology of the TiO_2 film dip-coated at the withdrawal speeds of 30 and 40 cm min^{-1} , respectively. From image (d), it is observed that the TiO_2 film begins to crack (in white rectangle), and it entirely cracked when the withdrawal speed was increased to 40 cm min^{-1} as shown in image (e). However, at high magnification, the SEM image of the TiO_2 film with withdrawal speed of 40 cm min^{-1} shows homogeneity (Fig. 4(e) inset). The SEM image of 50 cm min^{-1} withdrawal speed is not shown here because nano particles were literally seen to be removed from the substrate of the TiO_2 film. Fig. 4(f) shows the SEM image of five alternate coating/heating cycles of the TiO_2 film at 20 cm min^{-1} withdrawal speed, and it seems to have similar surface morphology as shown in the SEM images (b) and (c).

3.5. Photocatalytic test of TiO_2 films

The photocatalytic activity of the TiO_2 thin film, with/without surfactants assisted one coating deposited at 10 cm min^{-1} onto the pre-coated SiO_2 glass slides was evaluated by studying the degradation

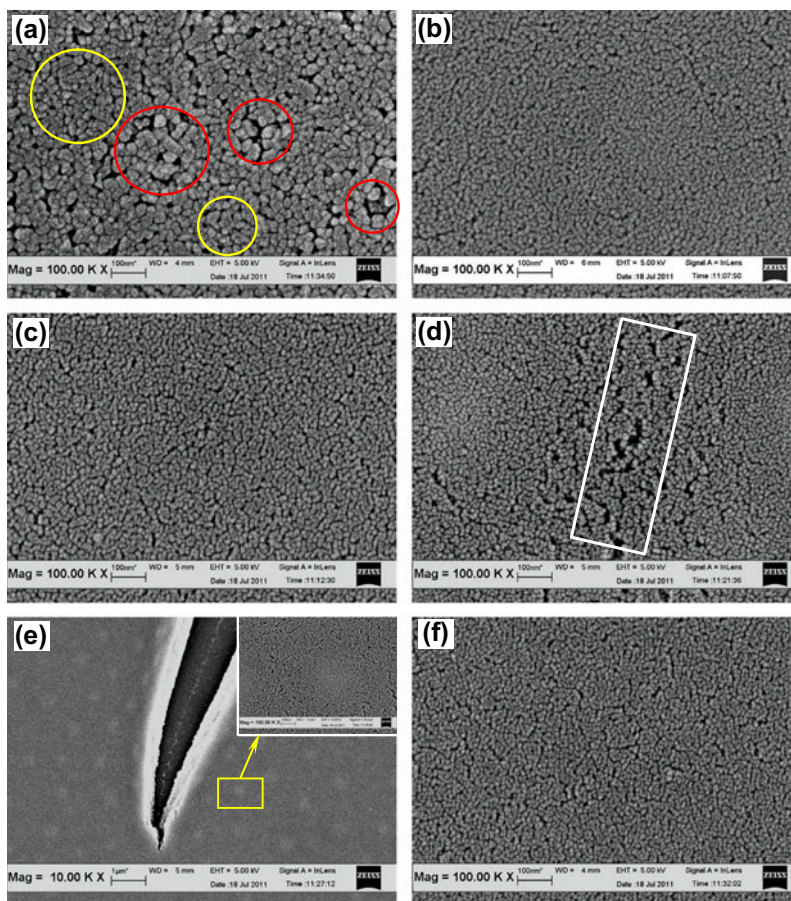


Fig. 4. SEM images of TiO_2 coatings with varying withdrawal speed: (a) without surfactant with 10 cm min^{-1} , (b–e) with surfactant assisted from 10 to 40 cm min^{-1} , and (f) five alternate dip coating on SiO_2 coated glass slide.

of RO16 in aqueous solution (25 mg L^{-1}) at an unadjusted solution pH of 5.54. Both photolysis and adsorption studies of the RO16 dye (Fig. 5) revealed that the dye is stable under UV light irradiation in the absence of a catalyst and equally does not have adsorption affinity to the catalyst surface as there was no color removal in either of the processes within 2 h. The effect of the surfactant was first analyzed for TiO_2 coatings. It is clearly seen from Fig. 5 that surfactant-assisted TiO_2 thin films resulted in faster degradation of RO16 dye than do the non-surfactant-assisted TiO_2 thin film. This is not only due to higher mass per unit area/thickness of film [20] but the synthesized coating belongs to mesoporous material [13]. Generally, it is known that, the higher the density of the coating, the smaller the contact area between the surface of the catalyst and the pollutant solution, and this acts to diminish the photocatalytic activity of the catalyst.

The generated mesopores help to enhance the photocatalytic activity of the film. Based on this

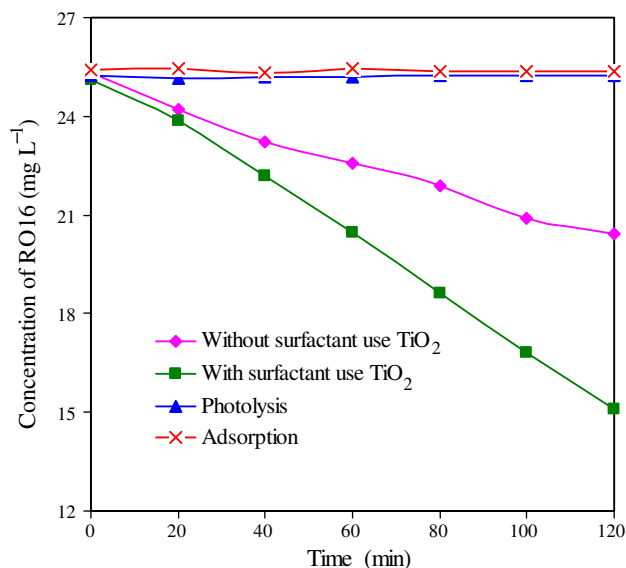


Fig. 5. Photocatalytic degradation of RO16 dye with TiO_2 and surfactant assisted TiO_2 film prepared with 10 cm min^{-1} withdrawal speed.

result, the surfactant-assisted film was selected for further studies.

3.6. Effect of withdrawal speed and alternate coatings on surface morphology and rate constant

Fig. 6 shows the interactive relationship that exists between the number of coatings and TiO_2 film thickness; number of coatings and rate constant for the degradation of RO16; withdrawal speed and TiO_2 film thickness; and withdrawal speed and the rate constant for the degradation of RO16. A close observation of Fig. 6 reveals a proportionate increase in film thickness as the number of coatings increased from one to six. This observation could be said to be true of the rate constant for the photocatalytic degradation of RO16 up to five coatings; thereafter the increase in the number of coatings to six did not seem to yield a proportionate increase in the rate constant. This result is a clear indication that there exists an optimum number of coatings after which further coating does not enhance the rate of degradation of RO16. (It has been reported that there is an optimum film thickness under which the rate of reaction is maximum because the fraction of light absorbed reaches 100% [38]. This statement could be true for dense thin film TiO_2 , but in the present investigation it is clearly articulated that the inner pores were blocked after a certain number of coatings; hence, increase in absorptivity did not yield any corresponding increase in the degradation rate. While the first observation is in perfect agreement with the findings of Yu et al. [34], the latter is not, because the

results of their findings indicated that there was a proportionate increase in rate constant (in the degradation of methyl orange) from 0.0189 to 0.0301 min^{-1} as the number of coatings increased from one to fifteen. A similar relationship as in the case of film thickness and the number of coatings, but with less TiO_2 film thickness was observed with varying withdrawal speeds from 10 to 50 cm min^{-1} . Specifically, when the withdrawal speed increased from 10 to 20 cm min^{-1} , a slight enhancement in rate constant was observed. But when further increase in withdrawal speed was made, there was almost double enhancement in the rate constant, and this could be linked to the increase in the surface area due to crack and pore formation in the film. Any further increase in the withdrawal speed beyond 40 cm min^{-1} was detrimental to the photocatalytic process, possibly because at such a high speed the coating would become so dense that it will crack and get removed during reaction. However, a comparison between the rate constants obtained at the $30/40 \text{ cm min}^{-1}$ withdrawal speed and two alternate coatings at 20 cm min^{-1} withdrawal speed reveals that an enhanced rate of degradation could be obtained with the film with two alternate coatings at 20 cm min^{-1} withdrawal speed with a uniform or crack-free surface morphology.

As noted earlier, there was no further improvement in the degradation rate constant for the TiO_2 thin film beyond five alternate dip-coated layers and this indicates that five alternate dip-coated is the optimum thickness of TiO_2 film within the confines of the present study for photocatalytic degradation RO16 dye. However, it was also confirmed from the UV-vis transmittance spectra of alternate TiO_2 coatings (Fig. 1(b)) that after five alternate coatings there was no significant enhancement in UV light absorption; but, the rate constant obtained for the five and six alternate coatings in the photocatalytic degradation of RO16 was almost the same. This result indicates that the porosity of the films increased up to five alternate coatings; thereafter the porosity of the inner coating is lost when further mesopore layer is coated on the glass slide. Therefore, increase in the dip-coating efficiency and light absorbance throughout the whole transparent film are possible factors for the slight enhancement in the light absorption, but no further enhancement in the photocatalytic activity beyond five alternate coatings of TiO_2 film was observed. It must be noted that the surface roughness of a material is directly proportional to its porosity, and it has previously been reported that there was no increase in the surface roughness of TiO_2 thin film after three or four coatings [19]. The referred report is in good agreement with the results of the present investigation. In the

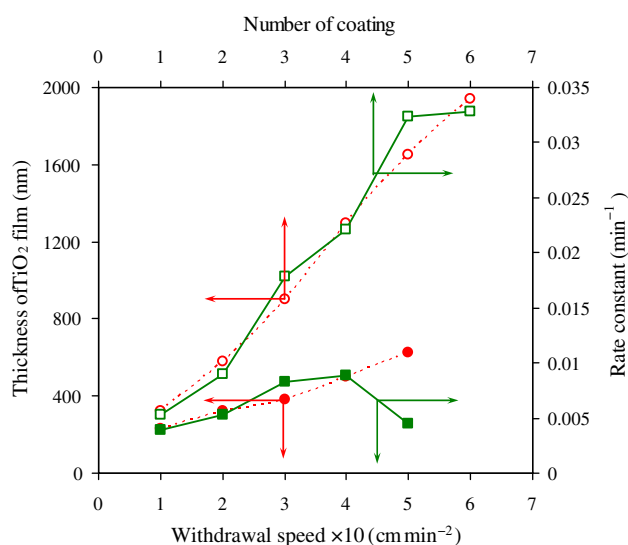


Fig. 6. Effect of withdrawal speed and alternate coatings on surface morphology and rate constant.

present study, it is clearly demonstrated that after five alternate coatings, there was a marginal increase in the degradation rate of RO16.

3.7. Reusability test on the alternate five TiO₂ coatings film

The reusability of the synthesized five alternate TiO₂ coatings' films was tested under the same experimental conditions. After every cycle, the five alternate TiO₂ coatings' films were withdrawn from the reactor, washed with double-distilled water, and dried at 50°C, and then reused in the photocatalytic degradation experiment. The results of four cycles are shown in Fig. 7. It is clear from the results that the efficiency of the five alternate TiO₂ coatings for the degradation of the RO16 is enhanced in each subsequent use up to the third cycle. The fourth cycle had almost the same percentage degradation as the third. Considering the same irradiation time of 120 min, only 64% degradation of RO16 dye was attained in the first use, whereas 97 and 99% degradation of RO16 were attained at the second and third cycles, respectively. A possible reason for the enhancement of the degradation efficiency in subsequent runs till the third cycle is that the films need some induction time to activate the photocatalytic process [18]. An induction period was also noticed with powder samples for the photocatalytic degradation of acid red 1 dye [9]. This induction time is also clear from Fig. 7 in the first use; within the first 60 min, only 12% RO16 dye was degraded. However, the second and third runs showed a great enhancement in the

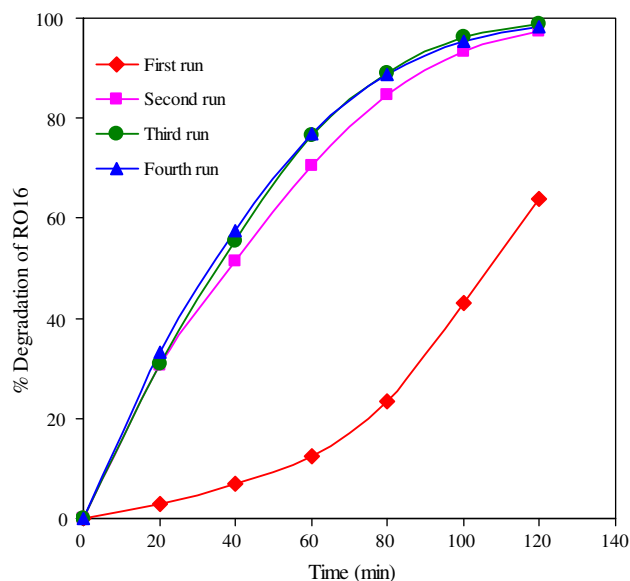


Fig. 7. Degradation of dye as a function of UV irradiation time and reproducibility of five alternate coatings response.

photocatalytic degradation of RO16 dye within the first 60 min reaction time. It can be seen from the Fig. 7 that 70 and 75% degradation of RO16 were achieved at the second and third cycles, respectively, as against 12% at the first use in 60-min irradiation time. This result indicates that induction time plays a vital role in elevating the amount of surface hydroxyl group and increasing the photocatalytic activity of five alternate TiO₂ coatings under UV light irradiation. UV light irradiation is needed for at least first 60 min for the enhancement in photocatalytic activity of five alternate TiO₂ coatings.

4. Conclusion

In the present work, a series of mesoporous TiO₂ thin films were prepared from weak acidic sol, which is stable for a couple of months. Thin films of surfactant- and non-surfactant-assisted sols were prepared and their photocatalytic activities tested in the degradation of RO16. The surfactant-assisted films showed a uniform distribution and reduced particle size compared to non-surfactant-assisted films. A 20 cm min⁻¹ withdrawal speed was found to maintain the films' surface uniformity up to five alternate coatings without cracking, whereas cracking started to occur at the withdrawal speed of 30 cm min⁻¹. The thin film fully cracked at 40 cm min⁻¹ withdrawal speed. Therefore, the best withdrawal speed for the present system is 20 cm min⁻¹. At 20 cm min⁻¹ withdrawal speed, mass per unit area of the film linearly increased with the number of coatings and the degradation rate remained constant for up to five alternate coatings. Further increase in the number of coatings to six did not show any significant increase in the degradation rate, though a slight UV light absorption was noticed. It could be concluded that five alternate coatings are sufficient for the model thin film and that further coatings resulted in the blocking of middle pores.

Acknowledgment

The authors acknowledge the research grant provided by the Universiti Sains Malaysia under the RU Grant Scheme (RU Grant No. 814005) and for granting the first author the privilege to undertake a post-doctoral program in the University.

References

- [1] R. Vinu, S. Poliseti, G. Madras, Dye sensitized visible light degradation of phenolic compounds, *Chem. Eng. J.* 165(3) (2010) 784–797.

- [2] R. Wang, K. Hashimoto, A. Fujishima, M. Chikuni, E. Kojima, A. Kitamura, M. Shimohigoshi, T. Watanabe, Light-induced amphiphilic surfaces, *Nature* 388 (1997) 431–432.
- [3] M. Ferroni, V. Guidi, G. Martinelli, G. Faglia, P. Nelli, G. Sberveglieri, Characterization of a nanosized TiO₂ gas sensor, *Nanostruct. Mater.* 7 (1996) 709–718.
- [4] C. Karunakaran, G. Abiramasundari, P. Gomathisankar, G. Manikandan, V. Anandi, Cu-doped TiO₂ nanoparticles for photocatalytic disinfection of bacteria under visible light, *J. Colloid Interface Sci.* 352 (2010) 68–74.
- [5] U.G. Akpan, B.H. Hameed, The advancements in sol-gel method of doped-TiO₂ photocatalysts, *Appl. Catal., A* 375 (2010) 1–11.
- [6] J. Zhu, J. Xie, M. Chen, D. Jiang, D. Wu, Low temperature synthesis of anatase rare earth doped titania-silica photocatalyst and its photocatalytic activity under solar-light, *Colloids Surf., A* 355 (2010) 178–182.
- [7] U.G. Akpan, B.H. Hameed, Photocatalytic degradation of 2,4-dichlorophenoxyacetic acid by Ca–Ce–W–TiO₂ composite photocatalyst, *Chem. Eng. J.* 173 (2011) 369–375.
- [8] T.S. Natarajan, M. Thomas, K. Natarajan, H.C. Bajaj, R.J. Tayade, Study on UV-LED/TiO₂ process for degradation of Rhodamine B dye, *Chem. Eng. J.* 169(1–3) (2011) 126–134.
- [9] U.G. Akpan, B.H. Hameed, Enhancement of the photocatalytic activity of TiO₂ by doping it with calcium ions, *J. Colloid Interface Sci.* 357 (2011) 168–178.
- [10] T. Yu, X. Tan, L. Zhao, Y. Yin, P. Chen, J. Wei, Characterization, activity and kinetics of a visible light driven photocatalyst: Cerium and nitrogen co-doped TiO₂ nanoparticles, *Chem. Eng. J.* 157 (2010) 86–92.
- [11] P. Wongkalasin, S. Chavadej, T. Sreethawong, Photocatalytic degradation of mixed azo dyes in aqueous wastewater using mesoporous-assembled TiO₂ nanocrystal synthesized by a modified sol-gel process, *Colloids Surf., A* 384 (2011) 519–528.
- [12] U.G. Akpan, B.H. Hameed, Solar degradation of an azo dye, acid red 1, by Ca–Ce–W–TiO₂ composite catalyst, *Chem. Eng. J.* 169 (2011) 91–99.
- [13] S.R. Patil, B.H. Hameed, A.S. Škapin, U.L. Štangar, Alternate coating and porosity as dependent factors for the photocatalytic activity of sol-gel derived TiO₂ films, *Chem. Eng. J.* 174 (2011) 190–198.
- [14] Z. Niu, F. Gao, X. Jia, W. Zhang, W. Chen, K.Y. Qian, Synthesis studies of sputtering TiO₂ films on poly(dimethylsiloxane) for surface modification, *Colloids Surf., A* 272 (2006) 170–175.
- [15] R.A. Damodar, T. Swaminathan, Performance evaluation of a continuous flow immobilized rotating tube photocatalytic reactor (IRTPR) immobilized with TiO₂ catalyst for azo dye degradation, *Chem. Eng. J.* 144 (2008) 59–66.
- [16] A.K. Ray, A.A.C.M. Beenackers, Development of a new photocatalytic reactor for water purification, *Catal. Today* 40 (1998) 73–83.
- [17] J. Zita, J. Krýsa, U. Černigoj, U.L. Lavrenčič-Štangar, J. Jirkovský, J. Rathouský, Photocatalytic properties of different TiO₂ thin films of various porosity and titania loading, *Catal. Today* 161 (2011) 29–34.
- [18] D. Barreca, A. Gasparotto, C. Maccato, E. Tondello, U.L. Štangar, S.R. Patil, Photoinduced superhydrophilicity and photocatalytic properties of ZnO nanoplatelets, *Surf. Coat. Technol.* 203 (2009) 2041–2045.
- [19] H. Yaghoubi, N. Taghavinia, E.K. Alamdari, Self cleaning TiO₂ coating on polycarbonate: Surface treatment, photocatalytic and nanomechanical properties, *Surf. Coat. Technol.* 204 (2010) 1562–1568.
- [20] S.R. Patil, U.L. Štangar, S. Gross, U. Schubert, Superhydrophilic and photocatalytic properties of Ag–TiO₂ thin film prepared by sol-gel technique, *J. Adv. Oxid. Technol.* 11(2) (2008) 327–337.
- [21] U. Černigoj, U.L. Štangar, P. Trebše, U.O. Krašovec, S. Gross, Photocatalytically active TiO₂ thin films produced by surfactant-assisted sol-gel processing, *Thin Solid Films* 495 (2006) 327–332.
- [22] Y. Chen, D.D. Dionysiou, Correlation of structural properties and film thickness to photocatalytic activity of thick TiO₂ films coated on stainless steel, *Appl. Catal., B* 69 (2006) 24–33.
- [23] P. Novotna, J. Krysa, J. Maixner, P. Kluson, P. Novak, Photocatalytic activity of sol-gel TiO₂ thin films deposited on soda lime glass and soda lime glass pre-coated with a SiO₂ layer, *Surf. Coat. Technol.* 204 (2010) 2570–2575.
- [24] Y. Ao, J. Xu, D. Fu, C. Yuan, Preparation of porous titania thin film and its photocatalytic activity, *Appl. Surf. Sci.* 255 (2008) 3137–3140.
- [25] D. Ishii, H. Yabu, M. Shimomura, Novel biomimetic surface based on a self-organized Metal–Polymer hybrid structure, *Chem. Mater.* 21 (2009) 1799–1801.
- [26] Y. Chen, E. Stathatos, D.D. Dionysiou, Microstructure characterization and photocatalytic activity of mesoporous TiO₂ films with ultrafine anatase nanocrystallites, *Surf. Coat. Technol.* 202 (2008) 1944–1950.
- [27] H. Choi, E. Stathatos, D.D. Dionysiou, Synthesis of nanocrystalline photocatalytic TiO₂ thin films and particles using sol-gel method modified with nonionic surfactants, *Thin Solid Films* 510 (2006) 107–114.
- [28] C. Han, M. Pelaez, V. Likodimos, A.G. Kontos, P. Falaras, K. O’Shea, D.D. Dionysiou, Innovative visible light-activated sulfur doped TiO₂ films for water treatment, *Appl. Catal., B* 107 (2011) 77–87.
- [29] Y. Chen, S. Lunsford, D.D. Dionysiou, Photocatalytic activity and electrochemical response of titania film with macro/mesoporous texture, *Thin Solid Films* 516 (2008) 7930–7936.
- [30] N. Negishi, T. Iyoda, K. Hashimoto, A. Fujishima, Preparation of transparent TiO₂ thin film photocatalyst and its photocatalytic activity, *Chem. Lett.* 24(9) (1995) 841–842.
- [31] J. Zhao, P. Wan, J. Xiang, T. Tong, L. Dong, Z. Gao, X. Shen, H. Tong, Synthesis of highly ordered macro-mesoporous anatase TiO₂ film with high photocatalytic activity, *Micropor. Mesopor. Mater.* 138 (2011) 200–206.
- [32] M. Bestetti, D. Sacco, M.F. Brunella, S. Franz, R. Amadelli, L. Samiolo, Photocatalytic degradation activity of titanium dioxide sol-gel coatings on stainless steel wire meshes, *Mater. Chem. Phys.* 124 (2010) 1225–1231.
- [33] M. Uzunova-Bujnova, R. Kralchevska, M. Milanova, R. Todorovska, D. Hristov, D. Todorovsky, Crystal structure, morphology and photocatalytic activity of modified TiO₂ and of spray-deposited TiO₂ films, *Catal. Today* 151 (2010) 14–20.
- [34] J. Yu, X. Zhao, Q. Zhao, Photocatalytic activity of nanometer TiO₂ thin films prepared by the sol-gel method, *Mater. Chem. Phys.* 69 (2001) 25–29.

- [35] H. Choi, E. Stathatos, D.D. Dionysiou, Sol-gel preparation of mesoporous photocatalytic TiO_2 films and $\text{TiO}_2/\text{Al}_2\text{O}_3$ composite membranes for environmental applications, *Appl. Catal., B* 63 (2006) 60–67.
- [36] R. Kavitha, S. Meghani, V. Jayaram, Synthesis of titania films by combustion flame spray pyrolysis technique and its characterization for photocatalysis, *Mater. Sci. Eng., B* 139 (2007) 134–140.
- [37] K.S.W. Sing, D.H. Everett, R.A.W. Haul, L. Moscou, R.A. Pierotti, J. Rouquerol, T. Siemieniewska, Reporting physisorption data for gas/solid systems with special reference to the determination of surface area and porosity, *Pure Appl. Chem.* 57(4) (1985) 603–619.
- [38] A. Mills, S.K. Lee, A. Lepre, I.P. Parkin, S.A. O'Neill, Spectral and photocatalytic characteristics of TiO_2 CVD films on quartz, *Photochemical Photobiol. Sci.* 1 (2002) 865–868.